



- **RESEARCH ARTICLE** -

Characterization and Construction of a Robust and Elastic Wall-Less Flow Phantom for High Pressure Flow Rate Using Doppler Ultrasound Applications

Ammar A. Oglat^{1,*}, MZ Matjafri¹, Nursakinah Suardi¹, Mohammad A. Oqlat², Ahmad A. Oqlat³, Mostafa A Abdelrahman³, O.F.Farhat¹, Muntaser S. Ahmad¹, Batool N. Alkhateb⁴, Sylvester J. Gemanam¹, Sabri M.Shalbi¹, Raed Abdalrheem¹, Marwan Shipli¹, Mohammad Marshdeh⁵

¹Department of Medical Physics and Radiation Science, School of Physics, Univirsti Sains Malaysia, 11800 Penang Malaysia

² Department of Biological Sciences, School of Science, Yarmouk University, Irbid Jordan

³ Faculty of Medicine, Department of emergency, JUST, Irbid Jordan

⁴ Faculty of Veterinary Medicine, JUST, Irbid Jordan

⁵ Department of Physics, College of Sciences, Al Imam Mohammad Ibn Saud Islamic University (IMSIU)

Abstract

A Doppler ultrasound is a noninvasive test that can be used to estimate the blood flow through the vessels. Presently, few flow phantoms are being used to be qualified for long-term utilize and storage with high physiological flow rate Doppler ultrasound. The main drawback of the two hydrogel materials items (Konjac (K) and carrageenan (C) (KC)) that it is not fit for long-term storage and easy to deteriorate. Thus, this research study focuses on the characterization and construction of a robust and elastic wall-less flow phantom with suitable acoustical properties of TMM. The mechanisms for the fabrication of a wall-less flow phantom utilizing a physically strong material such as K, C, and gelatin (bovine skin)-based TMM were explained. In addition, the clinical ultrasound (Hitachi Avius (HI)) system was used as the main instrument for data acquisition. Vessel mimicking material (VMM) with dimensions of 15.0 mm depth equal to those of human common carotid arteries (CCA) were obtained with pulsatile flow. The acoustical properties (speed of sound and attenuation were 1533 ± 2 m/s and 0.2 dB/cm. MHz, respectively) of a new TMM were agreed with the IEC 61685 standards. Furthermore, the velocity percentages error were decreased with increase in the Doppler angle (the lowest % error (3%) it was at 53°). The gelatin from bovine skin was a proper material to be added to KC to enhance the strength of TMM during for long-term utilize and storage of high-flow of blood mimicking Fluid (BMF). This wall-less flow phantom will be a suitable instrument for examining in-vitro research studies.

* Corresponding Author: Ammar A. Oglat, e-mail, ammar.oglat@yahoo.com

Keywords: BMF, TMM, Wall-less Flow Phantom, Acoustical Properties, Clinical Doppler Ultrasound (HI).

Article history:

Received 18 July 2018, Accepted 09 October 2018, Available online 10 October 2018
Introduction

Doppler ultrasound is a multifunction process used for measuring fluid (blood) flow with several applications such as evaluation degree of carotid narrowing (stenosis) (Grant et al., 2003; Oglat, Matjafri, Suardi, Oqlat, et al., 2018) and evaluation of pulsatility index (PI) through resistance measurement of downstream to flow (Chen, Pu, Liu, & Chiu, 1993). Evaluation and calculation of blood velocity (Bishop, Powell, & Rutt, 1986; Doucette et al., 1992), measuring and estimation of the wall shear stress as an indicator of atherosclerosis risk (Blake, Meagher, Fraser, Easson, & Hoskins, 2008; Brands, Hoeks, Hofstra, & Reneman, 1995; Kornet, Lambregts, Hoeks, & Reneman, 1998). Thus, the efficiency to precisely measure the blood flow velocity inside vessels is of magnificent value in research and clinical studies. However, to mimic the previous conditions for the proper definition of these quantities. The flow phantoms are the vital instruments for evaluation the novel methodologies (M. M. Oglat AA, Suardi N, Oqlat MA, Abdelrahman MA, Oqlat AA, et al. , 2018).

Wall-less flow phantoms provide a controllable method to examine and validate blood. The flow phantoms were fabricated for pre-clinical Doppler ultrasound 43 years back (Michie & Fried, 1973). Review articles related to blood flow methods were represented in 1989 (Law, Johnston, Routh, & Cobbold, 1989) and fabricate flow phantoms utilizing items is associated with the ultrasonic features of tissue was described in 2008 (P. R. Hoskins, 2008; M. M. Oglat AA, Suardi N, Abdelrahman MA, Oqlat MA, Oqlat AA. , 2018). The acoustical properties (speed of sound and attenuation) of TMM were evaluated, measured and found to be similar to the values and amounts of real human soft tissue and agreed with the International Electrotechnical Commission (IEC 2001) (Oglat et al.; Ramnarine, Anderson, & Hoskins, 2001). However, the main drawback of the KC-based TMM is that it is not adequate for long-term storage (Meagher, Poepping, Ramnarine, Black, & Hoskins, 2007).

As identified explicitly by the International Electrotechnical Commission (IEC 61685 standard 1999) (Browne, 2014; Commission, 2001), needs can be pleased by applying a proper BMF and TMM (S. N. Oglat AA, Matjafri Mz, Oqlat MA, Abdelrahman MA, Oqlat AA. , 2018). Usually, wall-less vessels are preferable in preventing mismatch problems in acoustic properties between TMM and the wall. It allows VMM to be appropriate because of the TMM direct link to the BMF and the removal of the Doppler artifacts (Browne, 2014).

In a flow phantom, the significant regard is to fabricate a vessel that is similar in physical dimensions (diameter and depth) with the real human vessel (in-vivo). In pre-clinical research studies, where the flow phantoms are being used to simulate the human to improve novel diagnostic mechanism before real clinical experiment on humans. The phantom vessel being studied are typically much larger than those in animals (mice and rats). Consequently, clinical Doppler ultrasound scanners should work at medium to high frequencies to supply the significant resolution (2–15 MHz). The pre-clinical flow phantoms can simulate the flow features within BMF vessels (Zhou, Kenwright, Wang, Hossack, & Hoskins, 2017). Therefore, the

fabrication design of wall-less flow phantom should be of great importance, because the rising in frequency leads to minimizing the penetration depth. Thus, this research study focuses on the characterization and construction of a robust and elastic wall-less flow phantom with suitable acoustical properties of TMM.

Elastography is a procedure that has ability to generate different modern sorts of images which is called elastograms. Accordingly, all the features of elastograms are different from the frequent features of sonograms. Thus, the main function of sonograms is to transfer data such as the acoustic backscatter power from TMM components, while the main function of elastograms is to convey data such as the Poisson's ratios (Young's moduli) and local strains. Typically, the parameters of elasticity are not immediately correlated with parameters of sonographic, for example, elastography transfers new data about internal structure of tissue (Ophir, 2002).

Material and Methods

Blood Mimicking fluid preparation

In this experimental research study, the target was to use a proper BMF with a suitable physical and acoustical properties. To get a new proper BMF, a proper mixture fluid which was prepared and made of distilled water 70.0 wt %, propylene glycol (PG) 5.0 wt %, and polyethylene glycol (PEG) (200 MW) 25.0 wt %, dispersed in spherical Poly (4-methylstyrene) scatters particle material 0.8 wt % was adopted in the BMF. The IEC standards values used were attenuation (< 0.1 dB/cm. MHz), speed of sound (1595 m/sec), density (1.04 g/ml), and viscosity (9.3 m Pa. s). The BMF was made of a suspension particle with a size of 3-8 μm and Poly (4-methylstyrene) particles materials in a PG/PEG (200 Mw) solution. The BMF was pumped and injected through a gear pump (GAMPT) before use to remove the clotting of powders particles for nearly 1 hour. And subsequently, degassed by a vacuum pump for nearly 1 hour before using it to get rid of air bubbles. The degassing and circulation process of BMF before use eliminated the spikes in the Doppler spectrum caused by large reflections from clots of the particles and air bubbles in the BMF (Oglat, Matjafri, Suardi, Abdelrahman, et al., 2018).

Those items or materials were 99% pure and supplies by Sigma Aldrich. The diameter of (Poly (4-methylstyrene)) particles is 3-8 μm , which determined by specific sieve in a unit of μm . Moreover, the PG and PEG were provided and supplied by Sigma Aldrich with suitable densities and molecular weight. The water in this experiment was obtained from medical physics and radiation science laboratory using a quartz distiller which produced distilled water for better performance.

Fabrication of Wall- Less Flow Phantom

Wall-Less Flow Phantom Construction

Fig. 1. displays a schematic graph of the wall-less flow phantom and the measurement set. An acrylic box was used as a container for the flow phantom. More so, small holes were drilled in both sides, and plastic pipe connectors were fixed and glued to site with epoxy (Araldite Rapid) material. For preventing movement of tissue at pipe side while applying the flow, the reticulated foam was used and glued near to the pipe connectors by epoxy. A metallic rod worked like a mold (form) for the phantom vessel (artery), with diameter size 8 mm, which is ideal for real

human CCA. The metallic rod was placed through the pipe connectors, and the pipe connectors were placed to make sure that the metallic rod is straight.

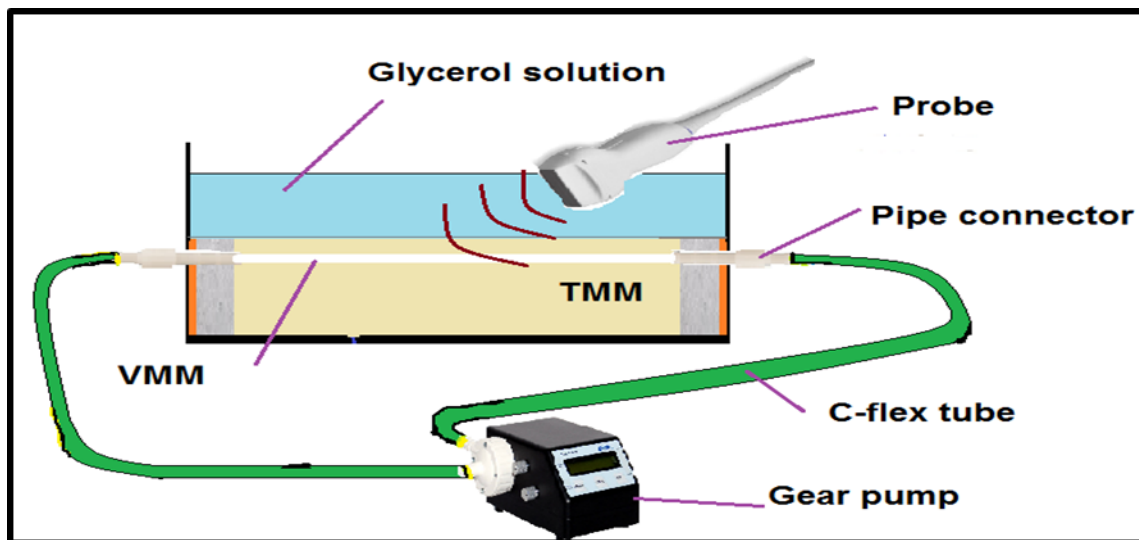


Figure 1. Schematic image of wall-less flow phantom.

Konjac Carrageenan (KC) are two organic items that become robust and flexible form when added together in water. In addition, the gelatin (bovine skin) helped to increase the strength of TMM. Powders used as scatter form with modifying grades supply the proper attenuation and speckle form. Also, the glycerol solution was added to make sure that the velocity of sound agrees that of real tissue. However, to get a proper flow phantom, manufacturing should be in a planned method with good-characterized and regular acoustic features. The attenuation and speed of sound of the TMM's were measured by using pulse echo (PE) method via A-scan ultrasonic (GAMPT) technique.

Fabrication of wall-less phantom

In this research study, the depiction of the fabrication of KC-based Wall-Less Phantom was explained. However, the phantom made of transparent acrylic, with the box opened from the top side of a house for the KC and gelatin-based TMM. Length, width, and height of this box are (260 mm X 120 mm X 90 mm) respectively with plastic pipe connectors and connected to flexible tubing to a container of BMF. A hard metallic rod (8mm) supplied a phantom mold for the artery (vessel) which was placed horizontally 15 mm beneath the scanning surface, because the ideal depth of real human CCA was achieved with pulsatile flow, with a depth of 15 mm, and due its significant to ensure that the relevant physical and acoustical features of this wall-less flow phantom which correspond to the features of real human tissues (Zhou et al., 2017). To the extent that when the TMM placed in the acrylic container and then the metallic rod immediately is removed, an artery bore is left in the TMM and allowed the BMF to pump through it. The diameter of the metallic rod determined the artery bore diameter, while the size of the container discovered the size of the phantom. The reticulated foam was used as a set factor of the TMM to the plastic pipe connectors to avoid leaking of the blood mimicking fluid. The schematic image of the fabrication method of wall-less flow phantom is shown in Fig. 2. The steps were described and mentioned as follows:

The plastic pipe (connectors) was required to be connected to each end of the acrylic container. In other words, they were stranded horizontally. At both sides of the acrylic container, two holes were drilled at the required depth of 50 mm and fixed the connectors in a suitable position with the rapid setting epoxy, then connected with flexible tubing to the outside area of the phantom.

- 1) The reticulated foam was glued near the pipes to make the TMM constant. Then, the metallic rod was inserted through the connectors at the required depth (50mm).
- 2) The KC-based TMM was poured into the mold to the desired depth level above the metallic rod. The metallic rod was removed slowly when the TMM was cooled. However, it was removed slowly to avoid twisting.
- 3) The BMF was injected through the flexible tube. Then, the flexible tube was connected to the gear pump from both sides.
- 4) The BMF did run and flow in the flow circuit for ten minutes to eliminate air bubbles and clotting in the system. The flow phantom at this step was ready for use.

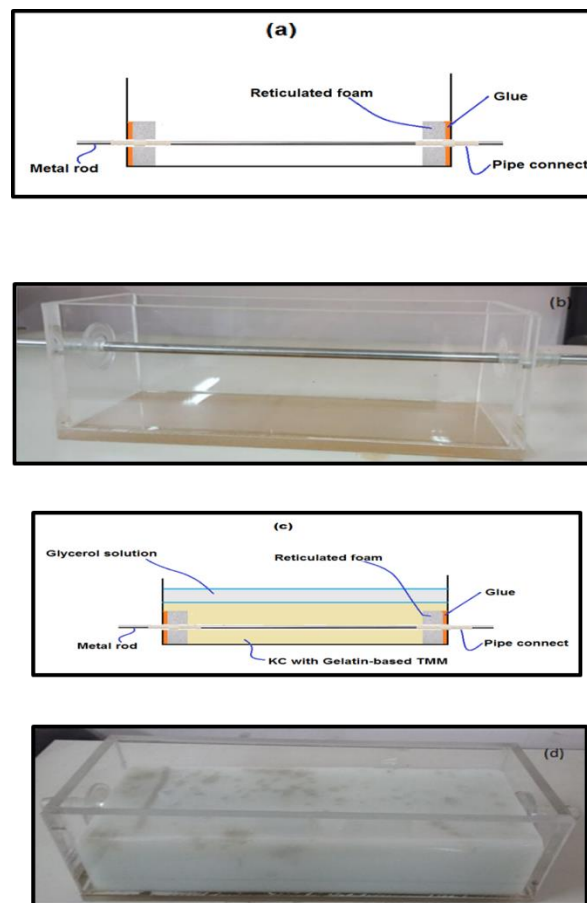


Figure 2. Schematic illustrations and photographs of the KC and gelatin-based wall-less phantom. 2a: Schematic illustration and 2b: photograph of empty vessel phantom mold ready for KC solution pouring. 2c: Schematic illustration and 2d: Photograph of vessel phantom (vessel diameter with 8 mm) with KC-based TMM and glycerol solution.

HI for Data Acquisition

A Digital clinical ultrasound scanner HI connected with linear array transducer EUP-L74M with focal clinical frequencies ranging from 5 to 13 MHz was utilized to collect ultrasound information and data from the wall-less flow phantom. The probe (transducer) was placed in an adaptable probe stand and the wall-less flow phantom on a suitable flat table. The probe was constant at a required angle and lowered near mostly to the surface of the wall-less flow phantom to prevent pressing the probe into the TMM. Because the CCA tube vessel is a straight and long tube, the BMF flow direction will be linear with the CCA tube axis, parallel direction to the tube vessel wall. The angle marker that appears on the keyboard was arranged with the direction of BMF flow. This angle is the angle between the beam produced by the ultrasound probe and the direction of BMF flow, as utilized in the ultrasound Doppler equation. The BMF velocity was measured with the HI clinical ultrasound scanner acting in PW-mode. The gate (sample) length adjusted to a suite with the entire vessel. The maximum velocity (V_{max}) in both the steady and pulsatile flow was measured by calculating the average maximum trace of the PW ultrasound Doppler signal utilizing a HI clinical ultrasound scanner keyboard software. CCA diameter was measured by taking the average of more than three measurements specified in B-mode Doppler ultrasound with the probe perpendicular to the artery (CCA) vessel. The KC with gelatin-based TMM was scanned by using B-mode ultrasound with different frequencies. In other words, the CCA vessel diameter was measured before, during, and after the flow. Due to the TMM elasticity, the change in CCA vessel diameter was noted while applying the flow. The inlet (cross-sectional) area of the tube connected to the gear pump and the cross-sectional of the vessel was measured and calculated by utilizing the diameter measurements while applying the flow.

Flow Rate and Confirming Parabolic (Laminar) Flow

The measurement values were utilized to evaluate the actual velocity (mean velocity) of the BMF through flow in the wall-less flow phantom by utilizing the flow rate formula (Kenwright, Laverick, Anderson, Moran, & Hoskins, 2015) Eq. (1).

$$Q_o = A_o \times V_o \quad (1)$$

Where Q_o is the flow rate volume

$$\begin{aligned} A_o & \text{ is the cross-section area of the tube} = \pi r^2 \\ & = \pi \frac{d^2}{4} \end{aligned}$$

d is the tube diameter

π is constant value = 3.14

V_o is the BMF velocity inside the vessel

To know the type of flow, for instance, turbulent or laminar flow, the Reynolds Number (R_e) must be calculated by measuring the entrance length (L_o) by following Eq. (2) (Kenwright et al., 2015; Zhou et al., 2016), and it must be less than 2100.

$$L_o = 0.04 \times d \times R_e \quad (2)$$

Where d is the size or diameter of the vessel, and Re is the Re , and it's unitless that specified by this Eq.:

$$Re = \frac{Dvd}{m} \quad (3)$$

Where D is the BMF density ($1040 \text{ kg/m}^3 = 1.04 \text{ g/cm}^3$), v is the BMF mean velocity (19.3 cm/sec), d is the vessel diameter ($8 \text{ mm} = 0.8 \text{ cm}$), and m is the BMF viscosity (9.3 mPa.s). To make sure that the developed flow was done completely, the measurements were turned out far away from the wall-less flow phantom entrance $> 2 \text{ cm}$. The investigation was turned out to be utilizing an 8.0-mm -diameter CCA vessel and L74M linear probe. The transducer was caught at a constant angle (53°) to the vessel, the lower gate (box) length was chosen (1.5 mm) and maximum velocity measurement was done. Note: the angle and sample length values were chosen regarding to normal CCA measurements (Grant et al., 2003; P. Hoskins, 2002; McNaughton & Abu-Yousef, 2011; Mehra, 2010).

The mean velocity resulted directly by Hitachi software and the PW spectral Doppler resulted by applying flow rate at 1125 ml/min via gear pump. This flow rate (1125 ml/min) resulted and calculated by using flow rate formula with average of flow velocity ($(30+35+40+45)/4 \text{ cm/sec}$) as an average values of normal velocity $30\text{-}45 \text{ cm/sec}$ of CCA velocity (Kenwright et al., 2015), that equals to 37.5 cm/sec .

Calculate the velocity Error Percentage of the Flow

For parabolic or laminar flow, the average or mean velocity is equal to half of the maximum or top velocity; Thus, the mean velocity was specified by Doppler ultrasound ($V_{\text{Doppler ultrasound}} = V_{\text{Top}}/2$). Doppler velocity measurements were done for a variety of angles. The actual mean velocity (V_{actual}) through the cross-sectional zone of the BMF was measured and calculated automatically by ultrasound device via timed collection. Velocity percentage error in blood flow was measured and calculated for each angle as:

$$\text{Velocity \% Error} = \frac{V_{\text{Doppler ultrasound}} - V_{\text{actual}}}{V_{\text{actual}}} \times \% 100 \quad (4)$$

By changing the angles and calculating the velocity percentage error, then plotting the result of percentage error against the beam objective angle. This process was pursued to gather data applying the linear available probe L74M.

Results and Discussion

The Pattern of Wall-Less Flow Phantom

Initial design

The TMM was prepared with KC alone. However, it was noted that the KC-based TMM was deformed with the continuous high pressure flow rate. Therefore, another TMM was desired to be qualified for long-term utilize and storage. The TMM rely on the hydrogels of konjac and carrageenan (Meagher et al., 2007), and a new robust material (gelatin) from bovine skin were added and utilized in this research study as a healthy alternative. However, these materials were used because they give proper acoustical properties (attenuation and speed of sound) in both the clinical and preclinical ultrasound studies. In other words, the acoustical features of KC and

gelatin-based TMM are suitable in the frequency range of the clinical and preclinical ultrasound 5–60 MHz (Kenwright et al., 2014). The gelatin (bovine skin) was mixed with KC-based TMM in four different ratios (1, 2, 3.5, and 5 g) to check and determine the effect of gelatin on the acoustical properties of the tissue.

The results obtained from the used of Konjac, carrageenan, and gelatin with bovine skin-based TMM were found to be strong, elastic, robust, and flexible material. The scatter factor of these materials by modifying grades provided the suitable attenuation and speckle pattern. In addition, adding glycerol to TMM mixture ensured that the acoustical properties agree with that of the tissue. Firstly, the acoustical properties of TMM that made without gelatin from bovine skin were agreed with the IEC 61685 standard, but the TMM was deformed with the continuous high flow. Thus, TMM of KC was made with the gelatin bovine skin because the acoustical measurements of TMM justified that the TMM was suitable for the Doppler application of research studies. The speed of sound and attenuation (acoustical properties) of KC with gelatin bovine skin -based TMM were 1533 ± 2 m/s and 0.2 dB/cm. MHz, respectively, a frequency range 1-10 MHz. The acoustical properties were measured using pulse echo (PE) mode via A-scan ultrasonic (GAMPT) technique.

Furthermore, the relationship between the speed of sound and concentration of gelatine from bovine skin is shown in Fig. 3. The result in the figure reveals that the speed of sound of TMM increased with increase in the gelatine from bovine skin concentrations. It implies that the gelatine from bovine skin could be a suitable factor to achieve proper acoustical properties of TMM. Also, the attenuation of all gelatine concentrations was <0.5 dB/cm. MHz.

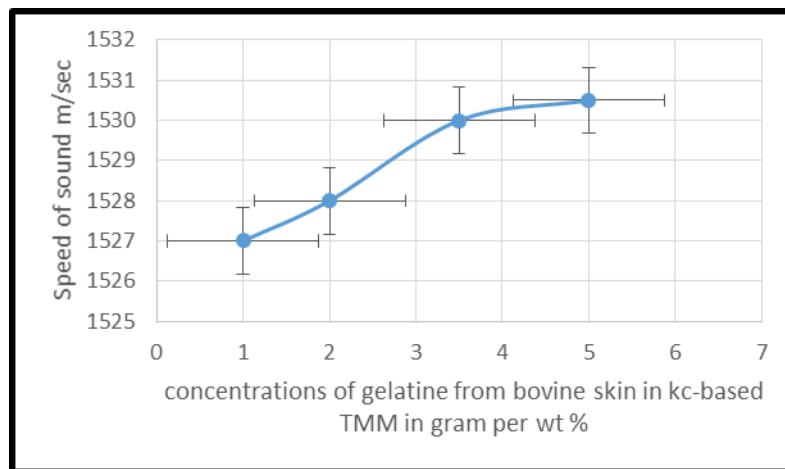


Figure 3. The relationship between speed of sound and percentage of gelatine from bovine skin.

However, in this research study, the making and utilizing of wall-less flow phantom proper for comparison to in-vitro ultrasound research studies such as CCA was discussed. The reliable performance of the Doppler measurements was obtained due to a suitable depth of vessel 15 mm or 1.5 cm from the scanning surface. Moreover, the small depth of the vessel helped to avoid TMM rupture during flow and with overtime (P. R. Hoskins et al., 2010). Although the benefits were due to the small depth of vessel, there are some drawbacks like the possibility of resistance mismatches at the vessel boundaries, and those boundaries cause refraction artifacts.

The Doppler ultrasound signals were obtained in good form because the attenuation of TMM was suitable according to the IEC-recommendations. And, for this reason, the C-Flex tubing like a VMM which has a speed of sound identical to human tissue wasn't used because the attenuation of C-Flex is nearly ten times greater than the tissue (Commission, 2001; P. R. Hoskins, 2008). Furthermore, the attenuation of C-flex tube avoids penetrating the ultrasonic beam to the depth and get a Doppler ultrasound signal with the probe under investigation. Because of the robust and strong nature of the TMM utilized in this research, a wall scanning was obtained with around 15 mm of TMM on the top surface, like the depth of a human CCA. Then, the removal of the attenuation issue could reduce mistakes linked with impedance mismatches of various materials.

The particular merit of the KC-Gelatin vessel flow phantom explained in this project is that it makes the physiologically worth environment for medical diagnostic Doppler ultrasound applications (imaging in the arterial). Thus, such well-fabricated wall-less flow phantom can be utilized for simulating the flow within the artery vessel.

Relationship between speed of sound and frequency

Table 1 enlist the speed of sound and standard deviation that calculated at a range of frequency (1-10 MHz). The average value was found to be 1533 ± 2 m/s as measured by the ultrasonic GAMPT systems. The results are found consistent with no significant differences in the studied frequency range (1-10 MHz). This is because the domain of the speed of sound does not change within the same medium even by changing the frequency (Sun et al., 2012). Furthermore, the standard deviation results show that the dispersion or variation of the group raw data values were low, and this indicates that the raw data points head for to be close to the average of the group.

Table 1. Speed of sound of the KC and gelatin-based TMM at different GAMPT probe frequencies.

Transducer sample frequency	Speed of sound (m/s)	Standard deviation SD
1 MHz	1533.1	0.013
2 MHz	1533	0.012
3 MHz	1533.1	0.026
4 MHz	1533.3	0.058
5 MHz	1533.2	0.058
6 MHz	1533.3	0.058
7 MHz	1533.4	0.058
8 MHz	1533.2	0.058
9 MHz	1533.3	0.058
10 MHz	1533.2	0.058

Relationship between attenuation and frequency

Fig. 4 presents the polynomial curve fitting for the total attenuation coefficient data which was set-up as a function of the frequency (1–10 MHz) by GAMPT probe. The results (Table 2) shows that there was a rapid increase in the attenuation measurements with increasing frequency. Typically, when the frequency increases the depth decreases and the attenuation increases (Sun et

al., 2012). Attenuation coefficient in the fluids and solids is proportional to the frequency. Moreover, the standard deviation results show that the dispersion or variation of the group raw data values were significant, and this indicates that the raw data points head for to be more than the average of the group.

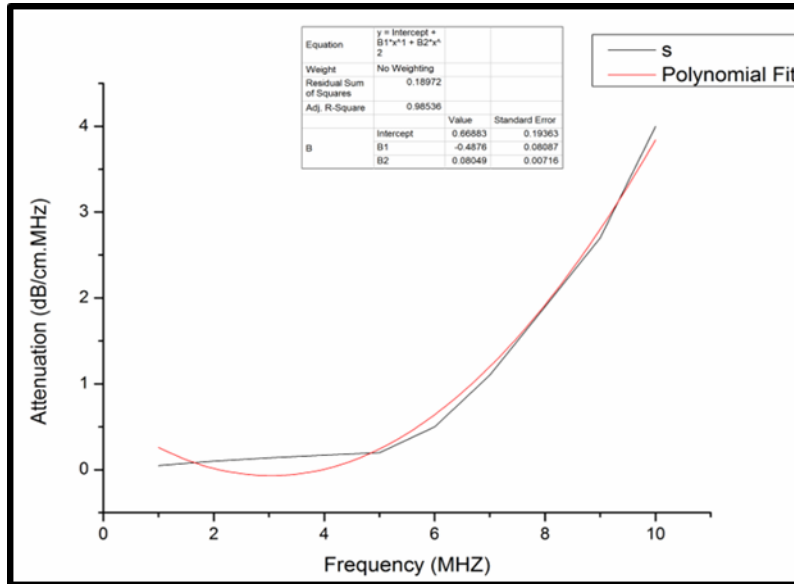


Figure 4. The polynomial curve-fit of the entire attenuation data set as a function of frequency measured by the GAMPT scanner in the frequency range of 1-10 MHz.

Table 2. Attenuation coefficient measurements of the KC and gelatin-based TMM at different GAMPT probe frequencies.

Transducer sample frequency	Attenuation coefficient dB/cm.MHz	Standard deviation SD
1 MHz	0.05	0.0039
2 MHz	0.1	0.058
3 MHz	0.14	0.01
4 MHz	0.17	0.007
5 MHz	0.2	0.014
6 MHz	0.5	0.031
7 MHz	1.1	0.06
8 MHz	1.9	0.05
9 MHz	2.7	0
10 MHz	4.0	0

In current study, the polynomial function was applied to the attenuation coefficient curve of the GAMPT probe since the attenuation coefficient of fluid displayed a proportional relationship to double of the frequency (f^2), and attenuation coefficient of TMM displayed to change linearly with frequency (Sun et al., 2012). This polynomial function $[Y(\alpha) = a + B1f + B2f^2]$ was found to be the best-fit for all the relevant attenuation vs. frequency data available for this TMM (1 to 10 MHz).

Bright-Mode (B-mode) Ultrasound Images

The KC-based TMM was scanned by using B-mode ultrasound with different frequencies and found that the B-mode image is showing tissue as grayscale due to the high signal intensity of echoes from the KC with gelatin-based TMM. Moreover, the resolution (brightness) was increased, suitable, and proper with increasing the frequency. Thus, the resolution nature of TMM images is mimic and simulate the resolution nature of real tissue. Additionally, the speckle pattern in all images was suitable and clear, because the items that used for making the TMM were suitable for clinical frequencies ranges 2-15 MHz and proper with the HI frequency (5-13 MHz). The lumen vessel is around 8 mm for this wall-less flow phantom.

Ultrasound B-mode images with and without applied the BMF flow were scanned of the vessel with an internal diameter of 8 mm comparable in diameter to a CCA. However, the average diameter of the inner vessel with applying the flow of BMF into the vessel is around 8.00 mm, and it is larger than the average diameter (7.73 mm) of the vessel without using the flow that was measured. Therefore, the vessel enlarges with flow inside the lumen vessel, due to the elasticity of the TMM. In addition, the TMM simulated the elasticity of real human tissue. The elasticity features of TMM are suitable to obtain biologically similar size changes through the pulsatile flow. It is very significant that the vessel diameter must be measured by applying the flow to prevent an over-evaluation of flow rate and to get on the proper calculation of flow amount from velocity measurements.

Pulse Wave-Mode (PW-mode) and Spectral Doppler Ultrasound

The images of PW spectral Doppler ultrasound mode were taken and presented with both steady and pulsatile flow to check the validation of the backscattering pattern of the BMF. However, in-vivo, the blood flow is typically pulsatile form in nature more than regular form (Ramnarine, Anderson, & Hoskins, 2001). Although the VMM required only pulsatile flow and the nature of flow in CCA is pulsatile, the image with the steady flow was taken to check the scattering pattern of the new BMF that was prepared.

Laminar (Parabolic) Flow and Velocity Outline

The Reynold number (R_e) was 17.3; it was considered as a normal range and no turbulence (trouble in the blood flow) signs because the R_e is less than 2100. The lowest inlet (entrance) length or diameter for BMF propagating at 19.3 cm/sec through a vessel diameter of 8.00 mm was 5.7 mm Fig. 5. However, the actual average velocity at 53° is equal to maximum velocity. Thus, the maximum velocity is $19.3 \text{ cm/sec} \times 2 = 38.6 \text{ cm/sec}$, this means that the BMF velocity at 1125 ml/min includes the normal range of CCA velocity 30-45 cm/sec.

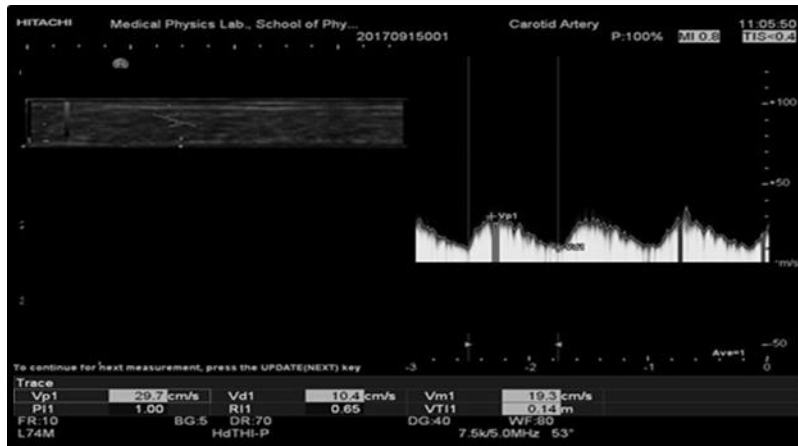


Figure 5. Mean velocity measurement of Doppler PW at a flow rate 1125 ml/min pumped by gear motor pump with Doppler angle (53°).

The velocity outline acquired from a wall-less flow phantom with a VMM diameter of 8.00 mm is shown in Fig. 6. The measurements were conducted by utilizing the L74M linear transducer, with the Doppler ultrasound angle of 53° to the VMM wall. The Doppler ultrasound angle of 53° was selected because of the velocity percentage error at the angle was minimal (3.0%). The resolutions were well at different frequencies; therefore, the ultrasound images can be scan at any frequency. The maximum velocity is positioned at the center of the VMM, decreasing to a lower value at the wall of VMM since the flow depends on the parabolic principle as shown in Fig. 7, the Doppler box (gate) adjusted to several different depths.

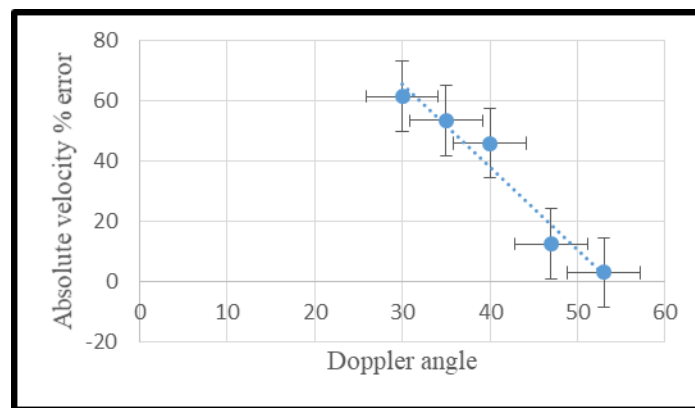


Figure 6. Percentage variation in the measured mean velocity of the BMF in the wall-less flow phantom as an action of beam–angle utilizing linear L74M ultrasonic probe working at 5.0 MHz and 8.00-mm-diameter wall-less flow phantom. In spite of valid modification of the Doppler ultrasound angle cursor, but there is rising variation between the true velocity and the measured mean velocity with changing the beam angle.

Figure 7. explains a parabola as a perfect form to the information in the formula $eD^2 + fD + g$ with a S^2 of 0.95. Where D is vessel wall depth measurements while e, f, and g are constants values. Furthermore, the main advantage of a parabola form of BMF flows inside the vessel is that it can measure the velocity at any place in the vessel. Nevertheless, the best point to measure

velocity is at the center of the vessel, and this is a significant consideration in wall-less flow phantom fabrication design. Such a value for the “actual” maximum velocity is evaluated from HI with the presumption of parabolic (laminar) flow. Moreover, the graph in Fig. 6 was used to determine the mean velocity of BMF which was increased at the center (sample length at the center of VMM) of VMM and decreased at wall side (sample length near to the wall of VMM and far from the center). Also, BMF flow is nearly parabolic or laminar. Thus, the maximum velocity is useable to evaluate the mean or average velocity.

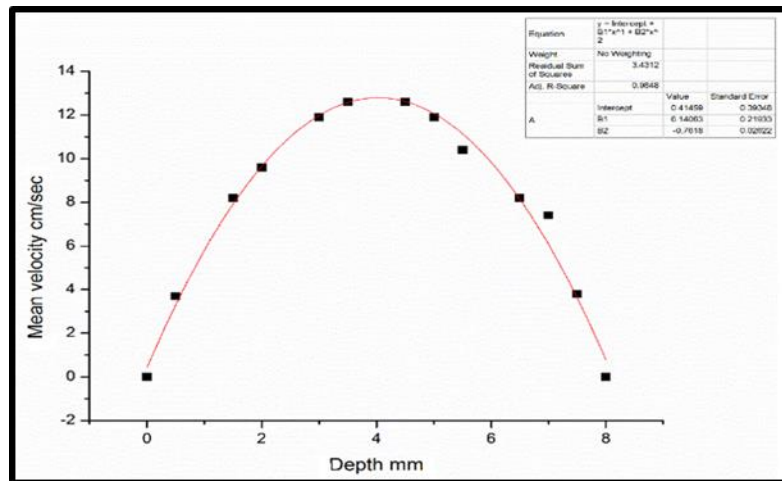


Figure 7. Velocity outline of BMF in an 8.00 mm wall-less flow phantom acquired utilizing the linear L74M probe acting at 5 MHz. The dashed spots or line is a laminar parabolic suitable to the data in the compose eD^2+fD+g with an S^2 of 0.95, where D is vessel wall depth measurements, while e , f and g are constants values. Since the BMF flow is nearly parabolic or laminar, thus, the maximum velocity is useable to evaluate the mean or average velocity.

Consequently, the flow outline of BMF through the phantom vessel suit a parabola, therefore, it can be said confidently that the BMF flow in the vessel phantom is laminar (Evans, 2000). The parabola principle in the design of the flow phantom is very important because the value for the “actual” maximum velocity was evaluated from the timed collection by the ultrasound device with a hypothesis of parabolic flow. In other words, there is perfect approval between the ultrasound velocity V_u/s and the “actual” velocity (V_{actual}) as specified from the flow rate measurements since the flow is a parabola and laminar.

Relationship between Doppler Angles and Velocity Error %

The effects of Doppler angles observed on the velocity percentage error. Graphs in Figure 6 were used to determine the percentage error of mean velocity with different Doppler angles. The absolute velocity percentage error was decreased with increasing the Doppler angle. The velocities percentage errors were %61.6, %53.6, %46.0, %12.5, %3.0, and %7.0 from the realistic value at 30° , 35° , 40° , 47° , 53° and 60° respectively. The result of this study shows and noted that it could be evaluated by 61.6%, with higher errors at 30 degrees (lower angles). Also, the minimum error % was at 53° , which means that at this angle the velocity measurements close to the optimum value. The best or the lowest value is which that is close to zero, because the error decreases when the value reaches close to zero.

Despite correct adjustment of the Doppler angle cursor, there is an increasing difference between the true velocity and the measured velocity with beam angle. The absolute velocity percentages error was resulted between the theoretical velocity and the ultrasound HI velocity with beam angle. Thus, the error in mean velocity it decreases with increase in the mean velocity due to an influence related to the probe utilization in sending and receiving the beam with a finite width. It implies that the mean velocity direction combines a range of Doppler angles which causes a propagation in the frequency with respect to the received signal (P. Hoskins, 1999). So, each probe has a specific focal width that can affect the velocity percentage errors. In this research study, it was noted that the L74M linear HI transducer helped to produce normal spectral broadening and decreased % error in spectral signal with increasing the Doppler angle even with enlarged the spectral signal (normal enlargement). Thus, applying of L74M Linear Probe was proper since the broadening of signal wave was normal. An investigation of mean velocity errors percentage applying various probes is out the scope of this research study.

Moreover, error % in the velocity with measurement Doppler angle noticed with the flow phantom is regular with geometric Doppler spectral broadening. In other words, the geometric Doppler spectral broadening was normal.

As can be seen in Figure 6, the best mean velocity was 19.3 at Doppler angle 53°, and the results were suitable because the sample length (box) was placed in the middle of the lumen artery. Since the best place of the sample length in normal CCA artery vessel is at the middle of the lumen in parallel direction to the artery vessel wall. And because the flow depends on the parabolic principle, the sample gate should be located at VMM center (Kenwright et al., 2015). While in an abnormal CCA it should be in parallel form to the trend of the blood flow. In addition, the result of the located sample length away from the vessel wall avoided the artificial spectral broadening.

Angle of Doppler Ultrasound

The Doppler angles that are suitable for Doppler measurements of the vessel were between 30 and 60, the top angle (80) being the upper permitted by the ultrasound scanner. While the minimum angle differs according to the scanner type because of a collection of both the focal width and focal depth and the width of the envelope surrounding the probe. In our project, the angles between 30° and 60° were the suitable field of Doppler angles to simulate the vessel (CCA) (Gerhard-Herman et al., 2006; Grant et al., 2003; Mehra, 2010). Mean velocity of BMF in the VMM was increased with Doppler angle increase, because when the theta increased the cosine theta decreased and then the mean velocity was increased. Moreover, blood velocity increased with Doppler angle because when Doppler angle increases, the beam of ultrasound become much aligned toward the direction of the flow and hence the velocity increases.

The top angle allowed via the HI was 80°, but it was not suitable for vessel measurements. Because the vessel simulates the CCA and the normal range of angles in CCA is between 30° and 60°, to minimize calculation errors and if the angle of CCA is more than 60° the measurements are less likely to be precise. Moreover, the lowest angle acquired by the HI was 0°, but also it was not a suitable degree for CCA Doppler ultrasound. Hence, there is a velocity result less likely to be precise at 0 degree (Grant et al., 2003; Mehra, 2010). However, when the Doppler angle increases from 0° to 60° the Cos angle decreases from 1 to 0.5. As the Doppler angle increases further to

90° from 60° the Cos angle decreases to 0 from 0.5 (McNaughton & Abu-Yousef, 2011). Regular utilization of an appropriate Doppler angle of effectiveness for speed measurements in the CCA decreases errors in speed measurements regarding the difference in the Doppler angle.

Stability and Long-period flow of the TMM

The efficiency of TMM made of KC and gelatin assessed and was suitable to resist the high continuous volume flow rates of BMF leakage. The geometrical constancy of the wall-less flow (TMM and VMM) styles were evaluated over 7 days of continuous of both the steady and pulsatile flow from 200-3000 mL/min. The 7 days were as a critical pointer of erosion or break-up the TMM over the full channel and withstood nearly 168 h of physiological flow over a 7-days period at specific temperatures ranging between 22°C and 39°C. The measurements of flow over a 7-days period were conducted by utilizing ultrasound B-mode with a 5-13 MHz linear array transducer (L74M) and found that there was no rupture of TMM and no leakage of BMF.

The cross-section and longitudinal area of the VMM displayed that no considerable variation over 7 days of continuous steady or pulsatile flow of 3 L/min. In other words, after 7 days of flow, there was no alteration in the physical measurements as specified from caliper measurements, in addition, the TMM surface was smooth and no rupture. And this is due to the robust, strong and elasticity of the TMM. However, the time was taken for the wall-less flow TMM styles to evaluate under the flow for 7 days is more than compare to the previous study which was taken 4 days then the tissue was ruptured (Ramnarine et al., 2001).

Constancy and suitability of wall-less flow phantom during high flow rate

Typically, the mean velocity of pulsatile blood flow in human vessels is lower than the steady flow, thus, as shown in Figures 8 and 9, the mean velocities of pulsatile flow were less than mean velocities of steady flow at the same flow rate. Consequently, at < 400 ml/min of the steady flow rate, the mean velocities could not be measured at < 600 ml/min of pulsatile flow rate. Because the flow was very weak inside large VMM and the device could not read it. Therefore, the HI frequency range (5-13 MHz) could not discover this low flow which is suitable to the small vessels or capillaries. Subsequently, the lowest detectable steady and pulsatile flow velocity were 400 ml/min and 600 ml/min, respectively. This case can occur in small arterioles or the capillaries with diameter <500 μm , and the flow can appear with perfusion case, and with high-frequency range (15-60 MHz).

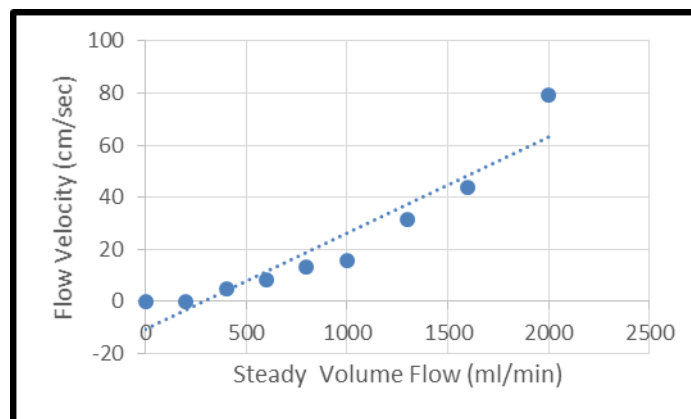


Figure 8. Mean velocity measurements for steady flow.

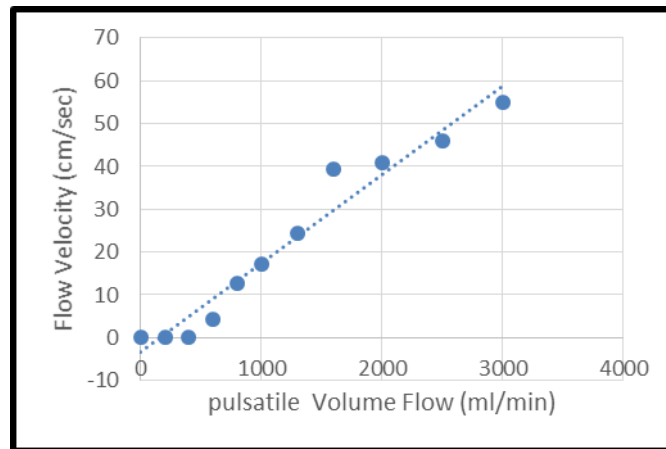


Figure 9. Mean velocity measurements for pulsatile flow.

Graphics plotted in Figures 8, and 9 were plotted to determine the mean velocity of BMF of pulsatile flow which was less than the steady flow at the same flow rate. Because the steady flow is a continuous process, while the pulsatile flow rises and decreases like a heart pump (lub dub).

Mean velocity was measured during applied several flow rates of steady and pulsatile blood flow through 8.0 mm. The mean velocity did not find a flow volume higher than 2000 ml/min as a steady flow and did not find a flow volume higher than 3000 ml/min as a pulsatile flow. Because the digital ultrasound (HI) could not read and register the very high values.

Moreover, the Figures determined that the TMM was strong and robust even with high BMF flow. Thus, the KC with gelatin-based TMM is suitable for high flow rate. The TMM do not change the form, and there was no shrinkage after 6 months of the fabrication. This may be due to chemical items such as glycerol with water which avoided the dehydration, and glucose since it increases the melting of gelatin in TMM in long-time. Thus, the acoustical properties do not change.

Conclusion

The comprehensive information about the steps for preparation of wall-less flow phantom items and fabrication of the Konjac and carrageenan with gelatine from bovine skin-based TMM of a wall-less flow phantom. In this study, useful methods, information, and receipt were designed for researches to fabricate and make ideally wall-less flow phantoms for their special medical Doppler ultrasound measurements.

Fabrication design of a wall-less flow phantom was proper and convenient for comparison to pre-clinical in-vitro research Doppler ultrasound. The percentage of velocity errors were calculated as a test trial for the wall-less flow phantom. Furthermore, the flow inside the VMM was with the laminar (parabolic) pattern. In other words, laminar (parabolic) pattern means that it's able to measure the BMF velocity at any depth of the vessel. The better useable Doppler

angle applying the available HI Ultrasound with L74M linear probe with this wall-less flow phantom was 53°, identical to angle attainable during in-vivo trials.

Further, the efficiency of TMM that made of KC and gelatin was assessed and suitable to resist the high-continuous volume flow rates of BMF leakage. However, the geometrical constancy of the wall-less flow TMM styles was evaluated over 7 days of continuous of both the steady and pulsatile flow from 200-3000 mL/min. The 7 days' time was a critical pointer of erosion or break-up the tissue mimicking material over the full channel. Also, the new flow phantom can be utilized and storage for long-term (several months (7-9 months)) if the care of the vascular wall-less flow phantom is taken to prevent exposition to atmospheric air by surrounding the TMM

The flow phantoms can be utilized for several months if the care of the wall-less flow phantom is taken to prevent exposition to atmospheric air by surrounding the TMM with 11.8% glycerol; 87.7% water; and 0.5% antifungal. The reticulated foam was used to avoid the leakage of BMF at high study or pulsatile flow, and to make sure that the TMM was sealed effectively. Further, the BMF and flow phantom can be utilized for diagnostic the normal CCA in-vitro by applying Doppler ultrasound.

Acknowledge

This research study was supported by Prof. Dr. Mohammad Zubir Mat Jafri, under the grant number 304/PFIZIK/6315023. We thank our colleagues from [Universiti Sains Malaysia, Medical physics and Radiation Science department] who provided insight and expertise that greatly assisted the research, although they may not agree with all of the interpretations of this paper.

References

- Bishop, C., Powell, S., & Rutt, D. (1986). Transcranial Doppler measurement of middle cerebral artery blood flow velocity: a validation study. *Stroke*, 17(5), 913-915.
- Blake, J. R., Meagher, S., Fraser, K. H., Easson, W. J., & Hoskins, P. R. (2008). A method to estimate wall shear rate with a clinical ultrasound scanner. *Ultrasound in medicine & biology*, 34(5), 760-774.
- Brands, P. J., Hoeks, A. P., Hofstra, L., & Reneman, R. S. (1995). A noninvasive method to estimate wall shear rate using ultrasound. *Ultrasound in medicine & biology*, 21(2), 171-185.
- Browne, J. E. (2014). A review of Doppler ultrasound quality assurance protocols and test devices. *Physica Medica*, 30(7), 742-751.
- Chen, J.-H., Pu, Y.-S., Liu, S.-P., & Chiu, T.-Y. (1993). Renal hemodynamics in patients with obstructive uropathy evaluated by duplex Doppler sonography. *The Journal of urology*, 150(1), 18-21.
- Commission, I. E. (2001). Ultrasonics—Flow measurement systems: Flow test object. *Draft IEC*, 1685.
- Doucette, J. W., Corl, P. D., Payne, H. M., Flynn, A. E., Goto, M., Nassi, M., & Segal, J. (1992). Validation of a Doppler guide wire for intravascular measurement of coronary artery flow velocity. *Circulation*, 85(5), 1899-1911.
- Evans, D. H. (2000). Doppler signal analysis. *Ultrasound in medicine & biology*, 26, S13-S15.

- Gerhard-Herman, M., Gardin, J. M., Jaff, M., Mohler, E., Roman, M., & Naqvi, T. Z. (2006). Guidelines for noninvasive vascular laboratory testing: a report from the American Society of Echocardiography and the Society for Vascular Medicine and Biology. *Vascular Medicine*, 11(3), 183-200.
- Grant, E. G., Benson, C. B., Moneta, G. L., Alexandrov, A. V., Baker, J. D., Bluth, E. I., . . . Hertzberg, B. S. (2003). Carotid artery stenosis: gray-scale and Doppler US diagnosis—Society of Radiologists in Ultrasound Consensus Conference. *Radiology*, 229(2), 340-346.
- Hoskins, P. (1999). A comparison of single-and dual-beam methods for maximum velocity estimation. *Ultrasound in medicine & biology*, 25(4), 583-592.
- Hoskins, P. (2002). Ultrasound techniques for measurement of blood flow and tissue motion. *Biorheology*, 39(3, 4), 451-459.
- Hoskins, P. R. (2008). Simulation and validation of arterial ultrasound imaging and blood flow. *Ultrasound in Medicine and Biology*, 34(5), 693-717.
- Hoskins, P. R., Soldan, M., Fortune, S., Inglis, S., Anderson, T., & Plevris, J. (2010). Validation of endoscopic ultrasound measured flow rate in the azygos vein using a flow phantom. *Ultrasound in medicine & biology*, 36(11), 1957-1964.
- Kenwright, D. A., Laverick, N., Anderson, T., Moran, C. M., & Hoskins, P. R. (2015). Wall-less flow phantom for high-frequency ultrasound applications. *Ultrasound in medicine & biology*, 41(3), 890-897.
- Kenwright, D. A., Sathoo, N., Rajagopal, S., Anderson, T., Moran, C. M., Hadoke, P. W., . . . Hoskins, P. R. (2014). Acoustic assessment of a konjac–carrageenan tissue-mimicking material at 5–60 MHz. *Ultrasound in Medicine & Biology*, 40(12), 2895-2902.
- Kornet, L., Lambregts, J., Hoeks, A. P., & Reneman, R. S. (1998). Differences in near-wall shear rate in the carotid artery within subjects are associated with different intima-media thicknesses. *Arteriosclerosis, thrombosis, and vascular biology*, 18(12), 1877-1884.
- Law, Y., Johnston, K., Routh, H., & Cobbold, R. (1989). On the design and evaluation of a steady flow model for Doppler ultrasound studies. *Ultrasound in medicine & biology*, 15(5), 505-516.
- McNaughton, D. A., & Abu-Yousef, M. M. (2011). Doppler US of the Liver Made Simple 1. *Radiographics*, 31(1), 161-188.
- Meagher, S., Poepping, T., Ramnarine, K., Black, R., & Hoskins, P. (2007). Anatomical flow phantoms of the nonplanar carotid bifurcation, part II: experimental validation with Doppler ultrasound. *Ultrasound in Medicine & Biology*, 33(2), 303-310.
- Mehra, S. (2010). Role of Duplex Doppler sonography in arterial stenoses. *Journal Indian Academy of Clinical Medicine*, 11(4), 294-299.
- Michie, D., & Fried, W. (1973). An in vitro test medium for evaluating clinical Doppler ultrasonic flow systems. *Journal of clinical ultrasound: JCU*, 1(2), 130.
- Oglat, A. A., Matjafri, M., Suardi, N., Abdelrahman, M. A., Oqlat, M. A., & Oqlat, A. A. (2018). A new scatter particle and mixture fluid for preparing blood mimicking fluid for wall-less flow phantom. *J Med Ultrasound*.
- Oglat, A. A., Matjafri, M., Suardi, N., Oqlat, M. A., Abdelrahman, M. A., & Oqlat, A. A. (2018). A review of medical doppler ultrasonography of blood flow in general and especially in common carotid artery. *Journal of Medical Ultrasound*, 26(1), 3.
- Oglat, A. A., Matjafri, M., Suardi, N., Oqlat, M. A., Oqlat, A. A., & Abdelrahman, M. A. A New Blood Mimicking Fluid Using Propylene Glycol and Their Properties for a Flow Phantom Test of Medical Doppler Ultrasound. *International Journal of Chemistry, Pharmacy &*

- Technology*, Vol. 2(No.5), pp-220-231, 2017.
- Oqlat AA, M. M., Suardi N, Abdelrahman MA, Oqlat MA, Oqlat A.A. (2018). A new scatter particle and mixture fluid for preparing blood mimicking fluid for wall-less flow phantom. *J Med Ultrasound*; {In press}.
- Oqlat AA, M. M., Suardi N, Oqlat MA, Abdelrahman MA, Oqlat AA, et al. . (2018). Chemical items used for preparing tissue-mimicking material of wall-less flow phantom for doppler ultrasound imaging. *J Med Ultrasound 2018* ; {In press}.
- Oqlat AA, S. N., Matjafri Mz, Oqlat MA, Abdelrahman MA, Oqlat AA. . (2018). A review of suspension- scattered particles used in blood- mimicking fluid for Doppler ultrasound imaging. *J Med Ultrasound*; {In press}.
- Ophir, J., Alam, S. K., Garra, B. S., Kallel, F., Konofagou, E. E., Krouskop, T., Merritt, C. R. B., Righetti, R., Souchon, R., Srinivasan, S., Varghese, T. . (2002). Elastography: imaging the elastic properties of soft tissues with ultrasound. *Journal of Medical Ultrasonics*, 29((4)), 155.
- Ramnarine, K. V., Anderson, T., & Hoskins, P. R. (2001). Construction and geometric stability of physiological flow rate wall-less stenosis phantoms. *Ultrasound in Medicine and Biology*, 27(2), 245-250.
- Sun, C., Pye, S. D., Browne, J. E., Janeczko, A., Ellis, B., Butler, M. B., Sboros, V., Thomson, A., Brewin, M., Earnshaw, C. H, Moran, M. C. (2012). The speed of sound and attenuation of an IEC agar-based tissue-mimicking material for high frequency ultrasound applications. *Ultrasound in Medicine and Biology*, 38(7), 1262-1270.
- Zhou, X., Kenwright, D. A., Wang, S., Hossack, J. A., & Hoskins, P. R. (2017). Fabrication of Two Flow Phantoms for Doppler Ultrasound Imaging. *IEEE transactions on ultrasonics, ferroelectrics, and frequency control*, 64(1), 53-65.
- Zhou, X., Xia, C., Khan, F., Corner, G. A., Huang, Z., & Hoskins, P. R. (2016). Investigation of ultrasound-measured flow rate and wall shear rate in wrist arteries using flow phantoms. *Ultrasound in medicine & biology*, 42(3), 815-823.